Distribution of the external pressure coefficients on the elliptic tower: experimental measurement compared with numerical modelling

Michal Franek[1,*], *Marek* Macák[2] and *Oľga* Hubová[3]

[1]Slovak University of Technology in Bratislava, Faculty of Civil Engineering, Department of Building Construction, Radlinského 11, 810 05 Bratislava, Slovak Republic
[2]Slovak University of Technology in Bratislava, Faculty of Civil Engineering, Department of Mathematics and Descriptive Geometry, Radlinského 11, 810 05 Bratislava, Slovak Republic
[3]Slovak University of Technology in Bratislava, Faculty of Civil Engineering, Department of Structural Mechanics, Radlinského 11, 810 05 Bratislava, Slovak Republic

Abstract. The wind flow around the elliptical object was investigated experimentally in the BLWT wind tunnel in Bratislava and subsequently solved by computer wind flow simulation. On a high-rise building model, the external wind pressure coefficients were evaluated for different wind directions and then compared with the numerical CFD simulation in ANSYS, where different models of turbulence and mesh types were used. The aim of the article was to evaluate and compare the obtained values and after analysing the results to choose the most suitable model of turbulence and mesh types, which showed the smallest deviations from the experimental values.

1 Introduction

At present, we are observing increasing trends in building of high-rise buildings of circular or elliptical shape. Similar trends can be seen in the construction of modern neighborhoods in Slovakia too. Since it is not possible to find information about the effects of wind on elliptical towers in the standards, it is necessary to carry out a detailed experimental and numerical analysis for a given type of structure. The vortices created behind the elliptical structure can cause a vibration perpendicular to the wind direction, similar to the Kármán effect. At higher wind speeds, a flutter may occur [1]. For that reason it is necessary to make specific wind study because the results from the Eurocode approach [2] can be inadequate. Codes do not offer the handling procedure for the elliptical building. Maximal negative values of the external pressure coefficient can reach higher values than from the codes specification [1]. First experiments of circular shapes were done by Strouhal in 1878. It is mentioned in publication of Zdravkovich [3]. Overall external pressures may be greatly increased when the building is in real conditions, such as in urban exposure [4].

* Corresponding author: michal.franek@stuba.sk

Many researchers [5-7] reported results from experimental investigation of pressure and force coefficient for various terrain conditions. Comparison between codes and practice offer many researchers too [8, 9]. Analysis of an elliptical cylinder by computational fluid dynamics (CFD) begins with the search for and improvement of turbulence models. The elliptical cylinder is also one of the important body objects in the CFD area where wind angle and aspect ratio are important parameters [10]. Basic research [11, 12] with experimental and numerical results is available for the flow past elliptical cylinder compared with other cylinders in laboratory conditions. But in currently available literature the authors did not find the interdisciplinary integrated experimental/numerical research of pressure distribution of the elliptic model in the building aerodynamics.

This work consists of an integrated experimental and numerical approach. These results may be useful for safe design, experimental and building practice. Results from the experimental measurement were used as a reference to calibrate the numerical model. Several turbulence models have been used to calibrate the numerical model. These approaches were compared and evaluated with the average and median error. The main issue in numerical model is to simulate correct Atmospheric Boundary Layer (ABL) with fully turbulent environment. Correct definition of the turbulence is difficult. It is more proper to express turbulence as a list of properties and attributes. It contains randomness, diffusivity, vorticity, scale spectrum, 3D structure, dissipation and non – linearity [13].

2 Experimental measurements

Boundary Layer Wind Tunnel (BLWT) in Bratislava was used to simulate the ABL and pressure distribution on the elliptical high-rise building. This type of wind tunnel works on a principle of negative pressure. Length of BLWT is 26.3 m, the test section is 2.6 m wide and 1.6 m high. It was necessary to reproduce correctly the roughness of the earth surface covering different terrain categories according to Eurocode [2]. Approaching flow can be varied between suburban and urban terrain conditions. To generate fully turbulent flow the wooden barrier 150 mm high and uniformly roughness field with dimpled foil 20 mm high had been used.

From measurement, the external pressure coefficient was calculated which is described as

$$c_{pe} = (p - p_s)/(0.5 \cdot \rho \cdot u^2) \tag{1}$$

where c_{pe} is external pressure coefficient (-), p is local surface pressure (Pa), p_s is free stream atmospheric or static pressure (Pa), ρ is density of air (kg·m^{-3}), u is longitudinal wind velocity at the top of tower (m·s^{-1}).

Pressure distribution was recorded with pressure transducer (Scanivalve DSA3217) with 16 temperature compensated piezoresistive pressure sensors with a pneumatic calibration valve. Sampling frequency for all pressure taps was 25 Hz and duration of measurement was 20 s.

2.1 Boundary conditions

Characterization of ABL in BLWT Bratislava according to Eurocode [2] belongs to category between 3 and 4. Before each experiment the properties of ABL were measured and checked such as longitudinal mean wind velocity profile, intensity of turbulence profile, integral length scale, non-dimensional power spectral density and aerodynamic roughness length. Illustration of mean wind profile and intensity of turbulence is in Fig. 1. During an experiment it was achieved the geometric (scaled), kinematic, dynamic similarity

in accordance with the recommendations of ASCE (American Society of Civil Engineers) [14].

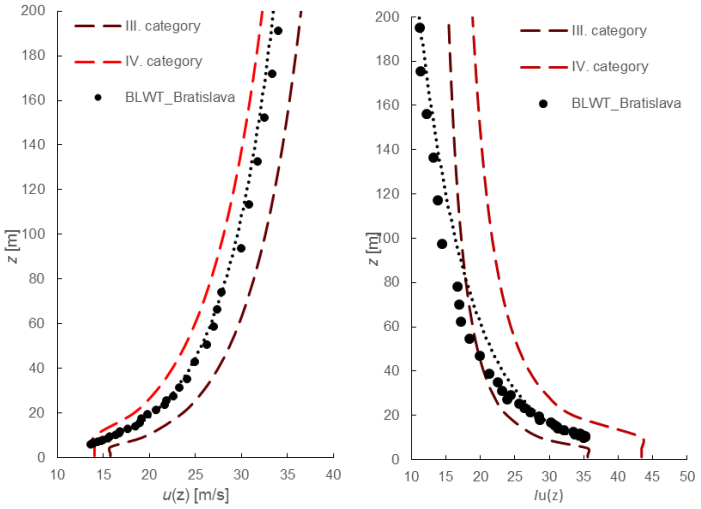

Fig. 1. Profile of mean wind velocity and intensity of turbulence.

2.2 Model of the elliptical tower

For pressure analysis and calibration with CFD model, the model of high-rise building with elliptical plan view was chosen. Ratio between width, length and height was 1:2.5:2.7. Model was made of plexiglass. It had 16 pressure taps with the same distance in 4 levels. For analysis only middle level was chosen. Illustration of the elliptical tower is in Fig. 2. Model was exposed to 0°, 45° and 90 ° angle of attack. Only zero angle was chosen to investigate the errors, because the aim of the article was to determine the accuracy of CFD for future study of the calibration process. These first fundamental results had shown us the critical part of CFD.

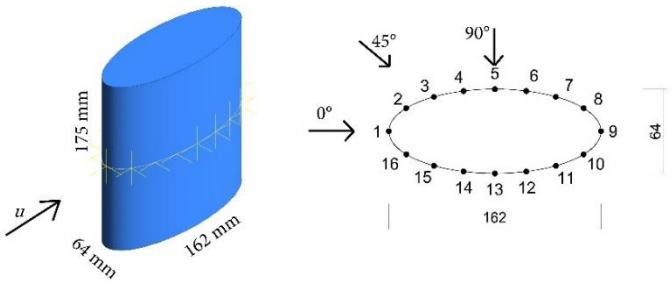

Fig. 2. Dimensions of the elliptical tower.

3 Numerical modelling

Results from the experiment were used as inputs for the simulation. ANSYS Fluent Workbench [15] was used to simulate similar approaching flow conditions and model of the elliptical tower as in experiment. The similarity with approaching wind profile in terms of mean wind velocity and turbulence intensity was as accurate as possible as it is illustrated in Fig. 3. Inlet boundary conditions of the domain are defined by the logarithmic

function. Intensity of turbulence is generated by equivalent sand-grain roughness height, which can be typed in ANSYS. Formulas for quantification of logarithmic function and roughness parameter are in Bert Blocken study [16]. To simulate real turbulent environment several turbulence models were used. They are solving the problem based on Navier – Stokes equations. Equations have mean and fluctuating value components. These values are derived from experimental and numerical solutions. $k - \varepsilon$ and $k - \omega$ turbulence models were chosen.

Size of computational domain was chosen to recommend maximum value of block ratio 3 % according to Stathopoulos [17]. The distance from elliptic tower to inlet, sides and top of the domain was at least five times the height of the tower and the distance from outlet was at least eleven times the height according to guidelines [17].

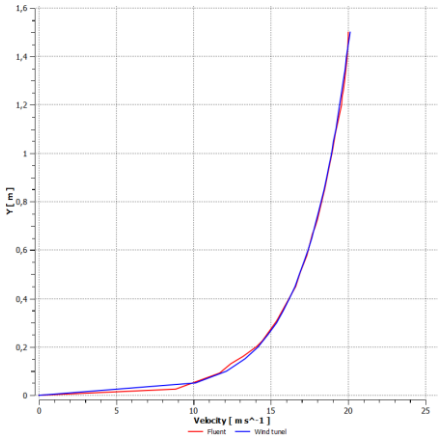

Fig. 3. Mean wind velocity profile from the experiment and the simulation.

From $k - \varepsilon$ model the RNG and Realizable models were chosen. Because the Reynolds number around an elliptic tower is low, RNG $k - \varepsilon$ model is useful for this case. It is derived from transport Navier – Stokes equations and has excessive diffusion for various circumstances, such as a big curving of the flow, eddies, rotation, separation of the flow and lower Reynolds numbers. Realizable $k - \varepsilon$ model is different from standard model. It has different formulation for modified transport equations and turbulent viscosity [18].

Second type of turbulence model was $k - \omega$ Standard and Shear – Stress Transport (SST). Standard model is more accurate in the vicinity of a wall but accuracy decreases with the distance. SST model converts $k - \varepsilon$ model to the accuracy in vicinity of a wall and works better in the free flow from the wall [19]. Transient state was used for each simulation process.

3.1 Meshing and simulation setting

Two types of meshing methods were used. First method was mesh with CutCell elements. Size of elements on the elliptic tower was 0.005 m. Second method was with polyhedral elements. For each meshing method advanced size function on curvature with fine relevance centre and high smoothing was used. Around 800 000 elements with 400 000 nodes were generated for each method. All used mesh methods are illustrated in Fig. 4 and Fig. 5

To obtain results similar with experimental part, the main task was to setup the simulation model and boundary conditions. It means the developed atmospheric boundary layer has the same logarithmic profile as in a wind tunnel and the profile is not deformed along the computational domain. This have been achieved by turbulence models, user

defined function and interpreted UDF function on inlet and outlet file and application of a roughness on the approach terrain.

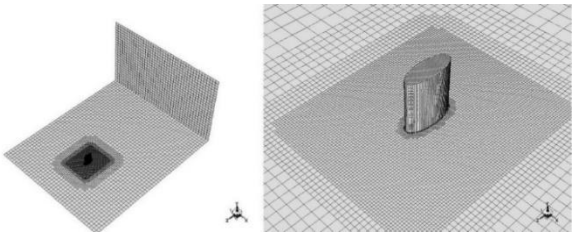

Fig. 4. CutCell elements mesh.

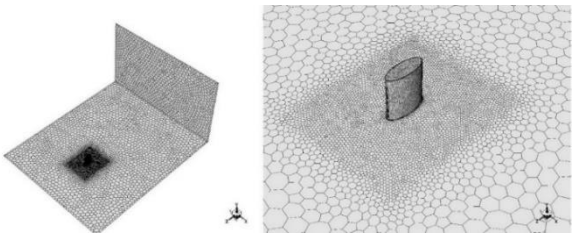

Fig. 5. Polyhedral elements mesh.

4 Results

Fig. 6 shows the c_{pe} values from the experiment and the simulation for each wind direction. The evaluation parameter of this work was the difference between the external wind pressure coefficients from the experiment and from the simulations at individual points on the model. In Table 1 and 2 there are values from experiment with minimal, maximal and mean value. Only average values were used to compare the match, as we only received mean values from the simulation. All values for middle level and 0 ° wind direction for various meshing methods and turbulence models are shown in Table 1 and 2. Errors were expressed in percentage. Resultant values of error were calculated as average and median.

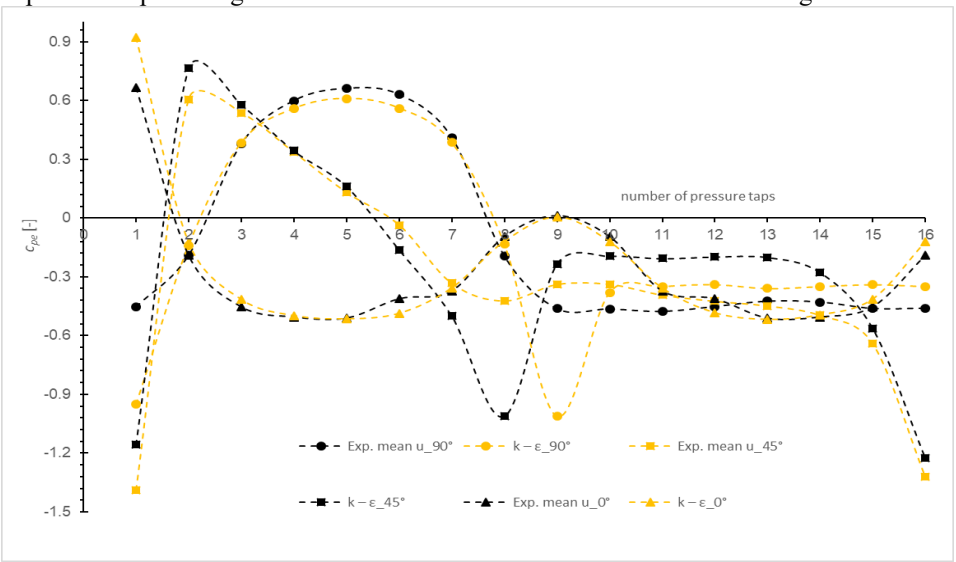

Fig. 6. Comparison between experimental and numerical approach.

Table 1. Comparison of results from experiment and CFD simulation – CutCell mesh.

Cutcell mesh											
Number of tap	Experiment			CFD							
	c_{pe}			*k-ε*				*k-ω*			
	Min	Max	Mean	RNG	**Error**	Realizable	**Error**	Standard	**Error**	SST	**Error**
1	0.25	1.08	0.67	0.93	**40%**	0.99	**49%**	0.99	**49%**	0.86	**29%**
2	-0.89	0.29	-0.19	-0.13	**32%**	-0.11	**41%**	0.08	**142%**	-0.15	**24%**
3	-0.91	-0.10	-0.45	-0.42	**7%**	-0.41	**9%**	-0.37	**17%**	-0.42	**7%**
4	-0.82	-0.25	-0.51	-0.50	**1%**	-0.50	**2%**	-0.50	**1%**	-0.50	**1%**
5	-0.80	-0.28	-0.51	-0.53	**3%**	-0.52	**2%**	-0.55	**7%**	-0.53	**3%**
6	-0.63	-0.23	-0.41	-0.50	**20%**	-0.50	**20%**	-0.53	**30%**	-0.50	**21%**
7	-0.57	-0.21	-0.37	-0.38	**2%**	-0.39	**5%**	-0.45	**22%**	-0.38	**1%**
8	-0.23	-0.01	-0.10	-0.13	**30%**	-0.16	**56%**	-0.17	**75%**	-0.15	**46%**
9	-0.15	0.08	-0.05	0.01	**120%**	0.02	**132%**	-0.03	**38%**	-0.08	**64%**
10	-0.23	-0.01	-0.10	-0.13	**30%**	-0.16	**55%**	-0.17	**75%**	-0.15	**46%**
11	-0.57	-0.21	-0.37	-0.38	**2%**	-0.39	**4%**	-0.46	**22%**	-0.38	**1%**
12	-0.63	-0.23	-0.41	-0.50	**20%**	-0.49	**20%**	-0.53	**30%**	-0.50	**21%**
13	-0.80	-0.28	-0.51	-0.53	**3%**	-0.52	**2%**	-0.55	**7%**	-0.53	**3%**
14	-0.82	-0.25	-0.51	-0.50	**0%**	-0.50	**2%**	-0.50	**1%**	-0.50	**1%**
15	-0.91	-0.10	-0.45	-0.42	**7%**	-0.41	**9%**	-0.37	**17%**	-0.42	**7%**
16	-0.89	0.29	-0.19	-0.13	**32%**	-0.11	**42%**	0.08	**142%**	-0.15	**24%**
				Average	**22%**		**28%**		**42%**		**19%**
				Median	**13%**		**15%**		**26%**		**14%**

Table 2. Comparison of results from experiment and CFD simulation – Polyhedral mesh.

Polyhedral mesh											
Number of tap	Experiment			CFD							
	c_{pe}			*k-ε*				*k-ω*			
	Min	Max	Mean	RNG	**Error**	Realizable	**Error**	Standard	**Error**	SST	**Error**
1	0.25	1.08	0.67	0.92	**38%**	0.97	**45%**	1.20	**80%**	0.81	**22%**
2	-0.89	0.29	-0.19	-0.13	**34%**	-0.12	**40%**	0.14	**173%**	-0.14	**28%**
3	-0.91	-0.10	-0.45	-0.42	**8%**	-0.41	**11%**	-0.37	**18%**	-0.40	**11%**
4	-0.82	-0.25	-0.51	-0.50	**1%**	-0.49	**3%**	-0.53	**5%**	-0.48	**5%**
5	-0.80	-0.28	-0.51	-0.52	**1%**	-0.51	**0%**	-0.59	**16%**	-0.50	**2%**
6	-0.63	-0.23	-0.41	-0.49	**18%**	-0.49	**18%**	-0.59	**44%**	-0.48	**17%**
7	-0.57	-0.21	-0.37	-0.36	**4%**	-0.37	**1%**	-0.51	**38%**	-0.37	**0%**
8	-0.23	-0.01	-0.09	-0.12	**26%**	-0.14	**50%**	-0.19	**102%**	-0.16	**70%**
9	-0.07	0.09	0.01	0.00	**65%**	0.01	**25%**	-0.01	**176%**	-0.01	**185%**
10	-0.23	-0.01	-0.09	-0.12	**28%**	-0.15	**54%**	-0.19	**98%**	-0.16	**68%**
11	-0.57	-0.21	-0.37	-0.36	**4%**	-0.37	**1%**	-0.52	**39%**	-0.37	**0%**
12	-0.63	-0.23	-0.41	-0.48	**17%**	-0.48	**17%**	-0.59	**44%**	-0.48	**16%**
13	-0.80	-0.28	-0.51	-0.52	**1%**	-0.51	**0%**	-0.59	**16%**	-0.50	**2%**
14	-0.82	-0.25	-0.51	-0.49	**2%**	-0.49	**4%**	-0.53	**5%**	-0.48	**5%**
15	-0.91	-0.10	-0.45	-0.41	**9%**	-0.40	**11%**	-0.37	**18%**	-0.40	**11%**
16	-0.89	0.29	-0.19	-0.12	**36%**	-0.11	**41%**	0.16	**186%**	-0.14	**30%**
				Average	**18%**		**20%**		**66%**		**29%**
				Median	**13%**		**14%**		**41%**		**14%**

5 Conclusions

Tables 1 and 2 compare and evaluate the errors of each simulation at each measurement point. The largest percentage differences occurred around points 8, 9 and 10 in an area with high turbulence and vortex shedding and low external wind pressure values for wind direction 0 °.

With changing the wind direction, the greatest differences occurred around points 8 and 9, in the vortex shedding areas, as shown in the graph in Figure 6. Because of the boundary conditions in CFD simulations, that consider zero wind pressure far beyond the model - at the exit of the area, these will not capture wind turbulence and vortexes just behind the model.

Results in Fig. 6 can show us, that bigger errors occur in higher values of pressure, especially in negative zone. If we do not take into account these values, errors seem quite accurate. It should be noted that these suction values are average and there is a big wind speed variation in these locations. For this reason, these areas are crucial, for example for cladding, dynamic response or pedestrian comfort.

It seemed that the turbulence model did not succeed to catch this turbulent environment. For that reason the overall mean error value was so large for each model and mesh. CFD follows the shape and behaviour of the experimental curve as it can be seen in Fig. 6, but areas with points of separation are shifted. CFD is not able to simulate real wind characteristics and boundary conditions just like an experiment and therefore it is not recommended to use only numerical results for design of an atypically shaped structure. Numerical approach can help us before experiment. CFD can help us find areas of extreme wind load values and determine positions of the sampling points before the experimental measurement. But the accuracy is still not sufficient.

The aim of this work was to analyze the accuracy of individual models of numerical simulation and to draw attention to the pitfalls that these procedures bring and to recommend the most suitable numerical model for a given object.

6 Future works

The aims for future work will be to find simulation setup for better similarity with experimental results in a wake area. Crucial factor will be to obtain stable and similar ABL with experimental setup. It means to create appropriate surface of a terrain and model with using of wall function or roughness height parameter. For this analysis, Reynolds Averaged Navier – Stokes (RANS) equation was used. Other possible way is to use Direct Numerical Simulation (DNS), which solves all the vortices/eddies. But it is very time-consuming with huge amounts of data.

This work was supported by the Scientific Grant Agency of the Ministry of Education, Science, Research and Sport of the Slovak Republic and the Slovak Academy of Sciences in the project VEGA 1/0113/19 and supported by the Slovak Research and Development Agency under the contract No. APVV-16-0126.

References

1. M. Franek, L. Konečná, O. Hubová and J. Žilinský, Experimental pressure measurement on elliptic cylinder, Appl Mech Mater. **820**, 332 – 337 (2016)
2. STN EN 1991-1-4: Eurocode 1: Actions on structures. Part 1-4: General actions. Wind actions (2007)

3. M. M. Zdravkovich, Different modes of vortex shedding: an overview, J. Fluids Struct. **10**, 427 – 437 (1996)
4. A. C. Khanduri, T. Stathopoulos and C. Bérard, Wind-induced interference effects on building – a review of the state-of-the-art, Eng. Struct. **20**, 617 – 630 (1998)
5. A. Abraham, P. Harikrishna, S. Selvi Rajan, G. Ramesh Babu, S. Chitra Ganapathi and M. Keerthana, Wind tunnel pressure measurement studies on 1:2:7 elliptic building model CSIR-SERC research report no. **R&D 01-MLP 18741-RR-04**, (2016)
6. E. Wiland, Unsteady Aerodynamics of Stationary Elliptic Cylinder in Subcritical Flow, M. A. Sc. Dissertation (1968)
7. N. J. Cook, (1990) *The designer's Guide to Wind Loading of Building Structures, Part 2 Static Structures*. (Butterworths, London, 1990)
8. Code of Practice for Design Loads (Other than Earthquake) for Buildings and structures—Part 3: Wind Loads, part 3 (1987)
9. Structural Design Actions, Part 2: Wind Actions AS/NZS: 1170.2:2011, Australian/New Zealand Standard (2011)
10. K. Shintani, A. Umemura and A. Takano, Low-Reynolds number flow past an elliptic cylinder, J. Fluid Mech. **136**, 277 – 289 (1983)
11. W. A. Khan, J. R. Culham and M. M. Yovanovich, Fluid flow around and heat transfer from elliptical cylinders: analytical approach, J. Thermophys Heat Transfer **19**, 178 – 185 (2001).
12. C. P. Jackson, A finite-element study of the onset of vortex shedding in flow past variously shaped bodies, J. Fluid Mech. **182**, 23 – 45 (1987)
13. B. Blocken and J. Carmeliet, A review of wind driven rain research in building science, J. Wind Eng. Ind. Aerodyn. **92**, 1079 – 1130 (2004)
14. ASCE Manuals and Reports on Engineering Practice, no. 67, Wind Tunnel Studies of Buildings and Structures. Library of Congress Catalog Card No.: 98-44103, USA, (1999)
15. ANSYS Inc., ANSYS Fluent Theory Guide, Release 18.1 (2017)
16. B. Blocken, T. Stathopoulos and J. Carmeliet, CFD simulation of the atmospheric boundary layer: wall function problems, J. Wind Eng. Ind. Aerodyn. **41**, 238 – 252 (2007)
17. T. Stathopoulos, H. Wu and C., Bedant, Wind environment around buildings, J. Wind Eng. Ind. Aerodyn **41-44**, 2377 – 2388 (1992).
18. D. C. Wilcox, Turbulence modelling for CFD, J. Fluid Mech. **289**, 460 (2006)
19. F. Menter et al., A correlation based transition model using local variables part 1 – model formulation, J. Turbomach. **128**, 2823 – 2838 (2004)